Quasi-Equilibrium AFM Measurement of Disjoining Pressure in Lubricant Nanofilms II: Effect of Substrate Materials

Adam P. Bowles,[†] Yiao-Tee Hsia,[‡] Paul M. Jones,[‡] Lee R. White,[†] and James W. Schneider*,[†]

Department of Chemical Engineering, Carnegie Mellon University, Pittsburgh, Pennsylvania 15213-3890, and Seagate Research Center, Seagate Technology, 1251 Waterfront Place, Pittsburgh, Pennsylvania 15222-4215

Received July 30, 2008. Revised Manuscript Received October 24, 2008

Atomic force microscopy (AFM) was used to measure the disjoining pressures of perfluoropolyether lubricant films (0.8−4.3 nm of Fomblin Z03) on both silicon wafers and hard drive disks coated with a diamondlike carbon overcoat. Differences in the disjoining pressure between the two systems were expected to be due to variations in the strength of van der Waals interactions. Lifshitz theory calculations suggest that this substrate switch will lead to relatively small changes in disjoining pressure as compared to the more pronounced effects reported due to changes in lubricant chemistry. We demonstrate the sensitivity of our AFM method by distinguishing between these similar systems.

Introduction

Disjoining pressure is of vital importance to the study of the liquid films present in foams, the liquid−liquid interfaces in surfactant stabilized emulsions, and the spreading of thin films on substrates.[1−3] Disjoining pressure is defined as the interaction energy change between two half-spaces as the thickness of intervening layers is varied.[4] It arises from a combination of van der Waals, electrostatic, and structural contributions.[5,6] The role of disjoining pressure is of considerable technological importance in the behavior of polymer films used as boundary lubricants for a hard drive's magnetic media.

Hard drive lubricants need to spread rapidly to prevent collision induced film defects from leaving the media susceptible to wear during subsequent record head-storage disk collisions. Previous researchers have linked the rheology of hard drive lubricants to disjoining pressure driven flow by solving the Navier−Stokes equation for spreading films.[7,8] The disjoining pressure is directly related to the chemical potential of the film, and by extension, the volatility of the lubricant in the film.[4] Additionally, the disjoining pressure dictates the lubricant films' stability or ability to spread uniformly across a surface.[9]

In this work, we use our previously described method for measuring the disjoining pressure of thin films into the megaPascal (MPa) range using atomic force microscopy (AFM).[10] This technique, originally developed by Mate and amplified by us, involves forming a liquid bridge between a film covered surface and an AFM probe.[11−14] If this meniscus is stretched (by pull-off of the tip from the substrate) at sufficiently small speeds, the Laplace pressure across the meniscus, ΔP, and the disjoining pressure, $\Pi(h)$, of the film approach equilibrium. Since true equilibrium can only be achieved in a static system, we refer to this approach to equilibrium as quasi-equilibrium.

$$\Delta P = -\Pi(h) \tag{1}$$

The Laplace pressure is given by

$$\Delta P \equiv -\frac{\gamma}{r_{\text{eff}}}; \quad \frac{1}{r_{\text{eff}}} \equiv -\left(\frac{1}{r_1} + \frac{1}{r_2}\right) \tag{2}$$

where γ is the surface tension of the air−lubricant interface, r_1 is the in-plane radius of curvature, r_2 is the axial radius as defined in Figure 2, and r_{eff} is the geometric average of r_1 and r_2. When the meniscus maintains equilibrium with the film, ΔP is a constant during pull-off and eq 2 may be used to find the theoretical pull-off force as a function of tip−sample separation with r_{eff} as the sole parameter.[11] By fitting the experimental retraction force curve to the theory curve, we determine r_{eff} (and hence $\Pi(h)$) for a given lubricant thickness, h.

Most research concerning head-disk interface lubrication focuses primarily on the effects of additives and polymer end group chemistry.[15−19] These approaches provide the most straightforward methods to dramatically alter the properties of the film including its disjoining pressure.[20,21] However, even incremental improvements in the properties of the overcoats and

* To whom correspondence should be addressed. E-mail: schneider@cmu.edu.
† Carnegie Mellon University.
‡ Seagate Technology.

(1) Bergeron, V.; Radke, C. J. *Langmuir* **1992**, *8*, 3020–3026.
(2) Binks, B. P.; Cho, W.-G.; Fletcher, P. D. I. *Langmuir* **1997**, *13*, 7180–7185.
(3) Claesson, P. M.; Ederth, T.; Bergeron, V.; Rutland, M. W. *Adv. Colloid Interface Sci.* **1996**, *67*, 119–183.
(4) Hsia, Y.-T.; Jones, P. M.; White, L. R. *Langmuir* **2004**, *20*, 10073–10079.
(5) Karraker, K. A.; Radke, C. J. *Adv. Colloid Interface Sci.* **2002**, *96*, 231–264.
(6) Derjaguin, B. V.; Churaev, N. V. *J. Colloid Interface Sci.* **1974**, *49*, 249–255.
(7) Karis, T. E.; Kim, W. T.; Jhon, M. S. *Tribol. Lett.* **2005**, *18*(1), 27–41.
(8) Ma, X.; Gui, J.; Grannen, K. J.; Smoliar, L. A.; Marchon, B.; Jhon, M. S.; Bauer, C. L. *Tribol. Lett.* **1999**, *6*, 9–14.
(9) Fukuzawa, K.; Shimuta, T.; Yoshida, T.; Mitsuya, Y. *Langmuir* **2006**, *22*, 6951–6955.
(10) Bowles, A. P.; Hsia, Y.-T.; Jones, P. M.; Schneider, J. W.; White, L. R. *Langmuir* **2006**, *22*, 11436–11446.
(11) Mate, C. M. *J. Appl. Phys.* **1992**, *72*, 3084–3090.
(12) Mate, C. M. *Phys. Rev. Lett.* **1992**, *68*, 3323–3326.
(13) Mate, C. M.; Lorenz, M. R.; Novotny, V. J. *J. Chem. Phys.* **1989**, *90*, 7550–7555.
(14) Mate, C. M.; Novotny, V. J. *J. Chem. Phys.* **1991**, *94*, 8420–8427.
(15) Gao, C.; Dai, P. *IEEE Trans. Magn.* **1997**, *33*, 3118–3120.
(16) Tagawa, N.; Tateyama, T.; Mori, A.; Kobayashi, N.; Fujii, Y.; Ikegami, M. *J. Tribol.* **2004**, *126*, 751–754.
(17) Zhang, H.; Mitsuya, Y.; Imamura, M.; Fukuoka, N.; Fukuzawa, K. *Tribol. Lett.* **2005**, *20*, 191–199.
(18) Kasai, P. H. *J. Inf. Storage Process. Syst.* **1999**, *1*, 23–31.
(19) Waltman, R. J. *Chem. Mater.* **2004**, *16*, 62–71.
(20) Tyndall, G. W.; Karis, T. E.; Jhon, M. S. *Tribol. Trans.* **1999**, *42*, 463–470.
(21) Jhon, M. S.; Phillips, D. M.; Vinay, S. J.; Messer, C. T. *IEEE Trans. Magn.* **1999**, *35*, 2334–2337.

10.1021/la8024638 CCC: $40.75
Published on Web 01/26/2009

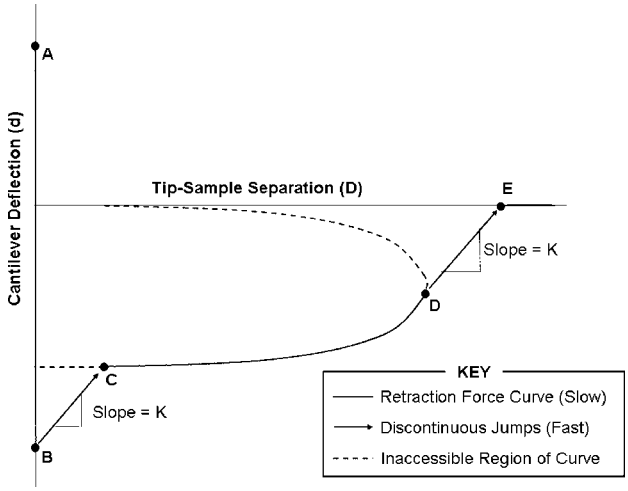

Figure 1. Qualitative example of an AFM retraction force curve collected by stretching a liquid bridge between a film-bearing surface and a spherical particle. A to B is observed when the tip and sample remain in contact. B to C is a cantilever mechanical instability leading to a quick jump out of tip−sample contact. C to D occurs when the liquid is suspended between the probe and film (the region of interest). D to E is a second instability resulting in a breakage of the meniscus.

lubricants on magnetic hard disks are of industrial importance. Thus, the technique must be sensitive to small changes in disjoining pressure due to minor changes in backbone, end group, or overcoat chemistry.

We have applied the AFM "pull-off" technique to films of the hard drive lubricant Fomblin Z03. Fomblin Z03 is a perfluoropolyether (PFPE) with MW = 4000 g/mol. It has the following structure:

$$CF_3-[O-CF_2-CF_2]_m-[O-CF_2]_n-O-CF_3$$

Films of Fomblin Z03 (about 0.5–5 nm in thickness) were prepared by dip-coating onto hard-drive platters having a diamond-like carbon (DLC) overcoat. We compared the measured disjoining pressures to Lifshitz calculations and to previous experimental results using silicon. Differences in $\Pi(h)$ upon switching substrates are expected to be caused primarily by changes in dispersive contributions to the disjoining pressure because polar components are reported to be relatively weak for film thicknesses above 0.4 nm.[22,23] For thinner films, electron donation from the ether oxygen on the backbone to the surface appears to be significant.[24−26]

No previous literature has directly compared the disjoining pressure or surface energy differences between Fomblin Z03 wetting a silicon surface and a hard disk with a DLC overcoat. Most studies present interactions in hard disk systems in terms of the surface energies measured by contact angle studies.[27−30] We have previously described the limitations of contact angle measurements in measuring surface energies.[4] Briefly, contact angle hysteresis prevents the measurement of accurate surface energies (using Young's equation) because of the invalid assumption that the three-phase line can instantaneously move to minimize free energy. Furthermore, interfacial behavior between the test film and the liquid probe is usually poorly understood. Calculation of accurate disjoining pressures using this method is unlikely, but contact angle measurements do offer qualitative insight into the interactions between the air and substrate half-spaces across the lubricant film. Therefore, previous contact angle literature for Fomblin lubricants could suggest how the Fomblin Z03 will behave differently on the hard drive overcoat (as compared to the silicon substrate).

Unlike Z03, most commercial lubricants display telechelic hydroxyl groups that bind strongly to hard-disk media (notably Zdol). We note that the structural similarity of Z03 and Zdol suggests that results from Z03 may approximate the dispersive component of the interaction of Zdol with DLC media. The dispersive component comes from decomposition of contact angle surface energies into polar and dispersive contributions by using polar and nonpolar wetting liquids and comparing the differences between the two. However, the limits of this approximation should be addressed. Contact angle experiments and modeling have been employed to measure the surface energies of Zdols and Z15 on amorphous carbon overcoats.[29,30] These studies show that the dispersive surface energy of Z-15 decreases more slowly (with respect to lubricant thickness) than that for either Zdol-2000 or 4000. In other words, the dispersive component of the disjoining pressure for Zdol is probably larger than that of Z15. This difference was attributed to structural effects induced by the Zdol end groups which forced the Zdol backbone to lie closer to the surface than the backbone of Z15 does.

Wu and Mate examined the effect of switching from silicon to an amorphous carbon substrate with Zdol.[28] In these experiments, they performed contact angle measurements on Zdol-4700 that reveal the silicon dispersive surface energy curve is shallower than that for the a-CH_x substrates, which means the silicon substrate most likely has lower disjoining pressures at all film thicknesses.

Waltman et al. used contact angle measurements for Zdol and Ztetraol on nitrogenated amorphous carbon (a-CN_x) to find the dispersive and polar components of disjoining pressure for these systems.[31,32] Their results for the dispersive term agree reasonably with our AFM disjoining pressure measurements for Z03 on a hard disk. They are slightly larger in both cases, and this may be caused by the aforementioned end group structural effect, the overcoat difference, or the hysteresis error. However, the relative agreement between these contact angle studies and our AFM data implies that their a-C overcoat behaves comparably to our DLC overcoats.

The similarity of amorphous carbon and DLC overcoats (relative to silicon) is further substantiated by Lifshitz calculations conducted by Dagastine et al.[33] The authors demonstrate via Hamaker functions that the expected progression of disjoining pressure would be a-C, DLC, and nitrogenated silicon in descending order. However, they show a-C and DLC terminated hard disks should have similar disjoining pressures while the nitrogenated silicon is separated by a significant margin. Dagastine et al. also present a Lifshitz calculation for a solely dispersive perfluoropolyether (PFPE) lubricant on a DLC overcoat at a very large head-disk spacing.[34] Their calculated disjoining pressure curve corresponds better with our data than any other published similar system.

There is a precedent for making disjoining pressure measurements of Z03 on silicon by AFM.[10,14,35,36] In most cases, the

(22) Chen, H.; Li, L.; Merzlikine, A. G.; Hsia, Y.-T.; Jhon, M. S. *J. Appl. Phys.* **2006**, *99*, 08N103-1–3.
(23) Chen, H.; Li, L.; Jones, P. M.; Hsia, Y.-T.; Jhon, M. S. *IEEE Trans. Magn.* **2007**, *43*, 2226–2228.
(24) Cornaglia, L.; Gellman, A. J. *J. Vac. Sci. Technol., A* **1997**, *15*, 2755–2765.
(25) Shukla, N.; Gellman, A. J.; Gui, J. *Langmuir* **2000**, *16*, 6562–6568.
(26) Paserba, K.; Shukla, N.; Gellman, A. J.; Gui, J.; Marchon, B. *Langmuir* **1999**, *15*, 1709–1715.
(27) Waltman, R. J.; Yen, B. K.; White, R. L. *Tribol. Lett.* **2005**, *20*, 69–81.
(28) Wu, J.; Mate, C. M. *Langmuir* **1998**, *14*, 4929–4934.
(29) Tyndall, G. W.; Leezenburg, P. B.; Waltman, R. J.; Castenada, J. *Tribol. Lett.* **1998**, *4*, 103–108.
(30) Waltman, R. J.; Tyndall, G. W.; Pacansky, J. *Langmuir* **1999**, *15*, 6470–6483.

disjoining pressures measured concur with those presented here,[10,35,36] with the disjoining pressure of the Z03 on silicon system being smaller than the dispersive contribution of Zdol on a carbon overcoat. The one reference that does not agree with the present data is the pioneering work done by Mate and Novotny.[14] This is likely due to their assumption of a linear relationship between the pull-off force and tip-sample separation. We have observed this does not hold for thicker films.[10]

Materials and Methods

Sample Preparation. Undoped silicon wafers (International Wafer Service) were cleaned for 20 min with a UV-ozone cleaner (Jelight Company) before film deposition. Hard drive platters (Seagate Technology) consisted of the layers shown in Figure 2. No cleaning step was performed on the hard disk surface. Lubricant was deposited on these surfaces by dip-coating them in a dilute solution of Fomblin Z03 (Ausimont USA) in Vertrel XF (Miller-Stephenson). Glassware used in preparation and storage of this solution was cleaned by soaking it in chromate solution (Fisher Scientific) for 15 min followed by rinsing with deionized water. The dip-coating apparatus employed was a KSV 5000 Langmuir−Blodgett film balance (KSV Instruments). Film thickness was controlled by varying the concentration of Fomblin in the immersion solution and the pull speed from the bath. Lubricant film thickness was identified using a Picometer ellipsometer (Beaglehole Instruments). Measurements for both bare and film-coated regions were taken far from the dipping interface of a half-coated substrate to prevent inaccuracies due to spreading of the film and the observed presence of a spike of lubricant at the interface (believed to be due to Marangoni flow at the initial dip interface). More than 20 readings were recorded in each region at equal spacings of 250 μm. From these, the average film thickness and an estimate of error were obtained.

Force Curve Measurements. A Multimode atomic force microscope (AFM) with a Nanoscope IIIa controller (Veeco Metrology) was used for force curve measurements. A PicoForce closed-loop control scanner (Veeco Metrology) was employed to minimize piezo drift. The cantilevers we used were reported to have a spring constant of 14 N/m. They were received from Novascan with a spherical silica particle of radius 0.5 ± 0.125 μm attached. The spring constants of the cantilevers were more accurately measured with the technique of Tortonese and Kirk using calibration cantilevers supplied by Park Scientific.[37] The cantilevers had widely varying spring constants with a mean of 11.94 N/m and a standard deviation of 2.66 N/m. The error for individual cantilevers from this method was estimated to be 4.50 N/m based upon uncertainty in the position of the AFM tip on the test cantilever and the mismatches in test-reference cantilever spring constants reported by Tortonese and Kirk. However, the large uncertainties remaining in the tip radius and spring constant were scaled out of the data as described in the Results and Discussion section. Prior to gathering data, these cantilevers were dipped in Vertrel XF and UV-ozone cleaned for 20 min to remove lubricant remaining from previous runs.

During experiments, the AFM was enclosed in a hood and the relative humidity maintained at less than 40%. Prior to this control, we observed that experimental force curves conformed to the constant Laplace pressure force curve model for relative humidities below 80%. In addition to the humidity hood, the instrument was insulated within a foam shroud for a period in excess of 18 h before force curve collection. This was done because a temperature-dependent drift was observed that we attribute to thermal expansion/contraction of the AFM itself. If not reduced, this drift was greater than the required retraction velocity for approach to equilibrium. By insulating the AFM, we heated it above ambient temperature until eventually a steady-state developed across the insulation. This dramatically reduced thermal drift and damped thermal shocks on the AFM system while gathering force curves. A residual tip−sample separation drift that was 0.02 nm/s or less was considered acceptable and was corrected for in the data analysis.

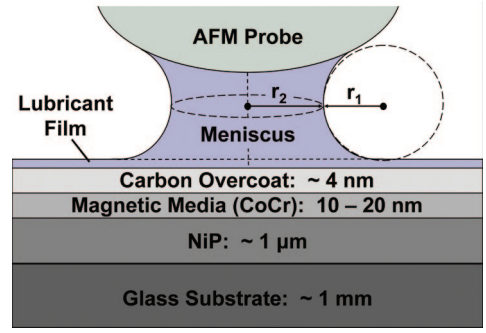

Figure 2. Schematic of the probe−film contact during an AFM retraction force curve. The parameters r_1 and r_2 represent the radii of curvature associated with the saddle-shaped meniscus stretched during one of these experiments. The layered substrate displayed is analogous to the hard disk surface used in these experiments.

To obtain force curves corresponding to the equilibrium condition, the probes were kept in contact with the film-bearing substrate for an extended period of time to allow lubricant to flow and wet the AFM tip (the wetting time). For most of the samples presented in this paper, a wetting time of 30 min was sufficient to bring the meniscus to equilibrium. The sole exception to this was the 3.9 nm Z03 film on silicon. A wetting time of 3 h was instituted for this larger, slowly filling meniscus. Following the wetting period, a retraction force curve was immediately performed. A constant retraction velocity of 0.0547 nm/s was used for each quasi-equilibrium pull-off curve.

Results and Discussion

To obtain reproducible quasi-equilibrium AFM force curves, the sensitivity of the AFM method to a number of experimental parameters must be determined. The relative sensitivity of the method to wetting time, tip radius, and retraction velocity is shown in Figures 3−5.

If an insufficient wetting time is used prior to force curve acquisition, pull-off curves will not extend to a long enough tip−sample separation to be described by the equilibrium model. This occurs because the meniscus has had inadequate time to fill to the equilibrium volume at contact. Wetting times are tested when unfamiliar substrates, lubricants, and film thicknesses are encountered to identify a correct tip wetting period. When a series of force curves with increasing wetting times is performed, the tip−sample separation increases until it approaches a limiting curve. This limiting curve is thought to be indicative of a tip that has been wetted to its equilibrium volume at contact. A suite of data demonstrating this behavior is shown in Figure 3. Approach to the limiting curve is judged to have been attained by 30 min.

Another consideration is the effect of prior experiments on the tip wetting in subsequent trials. Excess lubricant (relative to equilibrium at tip−sample contact) could remain on the AFM probe from previous experimental runs and lead to an underestimate of the correct disjoining pressure isotherm. This excess lubricant would likely be drained during the wetting step prior to the next force curve, but we take additional care to remove

(31) Waltman, R. J. *Langmuir* **2004**, *20*, 3166–3172.
(32) Waltman, R. J.; Khurshudov, A.; Tyndall, G. W. *Tribol. Lett.* **2002**, *12*, 163–169.
(33) Dagastine, R. R.; White, L. R.; Jones, P. M.; Hsia, Y.-T. *J. Appl. Phys.* **2005**, *97*, 126106-1–3.
(34) Dagastine, R. R.; White, L. R.; Jones, P. M.; Hsia, Y.-T. *J. Appl. Phys.* **2005**, *98*, 124906-1–6.
(35) Fukuzawa, K.; Kawamura, J.; Deguchi, T.; Zhang, H.; Mitsuya, Y. *J. Chem. Phys.* **2004**, *121*, 4358–4363.
(36) Jones, P. M.; Luo, M.; White, L. R.; Schneider, J.; Wu, M.-L.; Platt, C.; Li, L.; Hsia, Y.-T. *Tribol. Int.* **2004**, *38*, 528–532.
(37) Tortonese, M.; Kirk, M. *Proc. SPIE−Int. Soc. Opt. Eng.* **1997**, *3009*, 53–60.

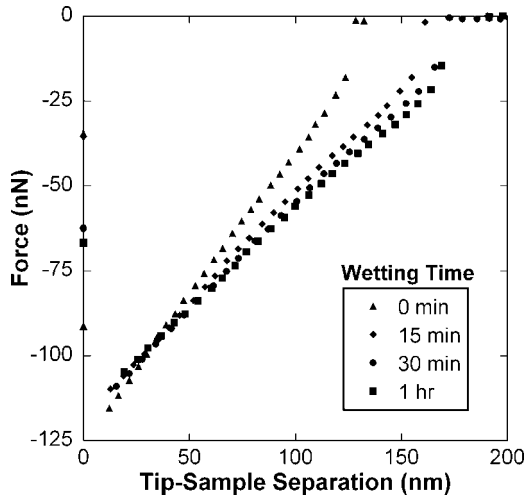

Figure 3. AFM data from a 1.8 nm PFPE film deposited on silicon taken at a retraction velocity of 10 nm/s. Increasing curve length is due to longer tip−sample contact times prior to force curve collection. Extended contact times allow more lubricant to flow into the meniscus on the AFM probe.

residual lubricant between force curves by immersing the cantilevers in Vertrel XF and UV-ozone cleaning them as described in the Materials and Methods section. The efficacy of this method has been tested by depositing Fomblin Z03 on a silicon wafer with a native oxide layer (as an analogue for our particle) and measuring the amount of lubricant on the wafer before and after the cleaning step using ellipsometry. The ellipsometry experiment confirms that the Z03 is removed following the cleaning step. Repeated probing of a surface could also lead to film depletion on the substrate due to lubricant transfer to the swelling meniscus. We consciously avoid regions of a sample that have been examined before, but a simple calculation reveals that the probability of landing within the depletion region of a previous experiment is, in a worst case scenario, less than 0.005%.

The spherical particle radius, R, of 0.5 μm was selected as optimal for the samples. The small size of the sphere allowed it to quickly reach equilibrium due to the minimal volume entrained in the bridge. The particle was also an appropriate size to sample industrially relevant lubricant thicknesses for both substrates. Thick films will engulf a tip (as shown in the Figure 4 inset) violating the conditions of the force curve model, a situation we refer to as tip flooding. We have calculated that tip flooding should occur when[10]

$$\frac{r_{\text{eff}}}{R} \cong 2.53 \tag{3}$$

Figure 4 shows a comparison of 4.3 and 4.8 nm Z03 films on hard disk surfaces examined using identical conditions (including the same tip). A dramatic change in behavior is seen with only a moderate difference in film thickness. This behavior is believed to be caused by tip flooding. The effective radius of the 4.8 nm film is estimated as $r_{\text{eff}} = 1036$ nm from extrapolation of a power law fit of the AFM disjoining pressure data presented later. Minimum and maximum values for r_{eff} obtained by a power law fit of the error bar extrema give us a range of 928−1183 nm. Using the upper and lower bounds for both r_{eff} and R,

$$1.48 < \frac{r_{\text{eff}}}{R} < 3.15 \tag{4}$$

This reveals tip flooding as possible for this sample. For the 4.3 nm film, we obtain the bounds

$$0.94 < \frac{r_{\text{eff}}}{R} < 2.11 \tag{5}$$

making attainment of the flooding condition unlikely.

Figure 5 shows the effect of lubricant fluid flow during the force curve. If the retraction velocity of the stage used for the force curve is too fast, the meniscus is stretched so quickly that lubricant does not have time to drain (violating the equilibrium condition). This results in force curves that extend to larger tip−sample separations than expected. A velocity of 0.0547 nm/s was selected because a convergence to a limiting curve (as in Figure 3) is observed as retraction velocity of the stage is decreased. Again, this data suggests realization of equilibrium.

The experimental force curve data were scaled by the force at the tip−sample contact point, $F(0)$, before being fitted with the theoretical model. This scaling reduced the effect of uncertainty in tip size (∼25%) and cantilever spring constant (∼37%) on the fitting process, leading to superior agreement between the data and theory. Fitting the data allowed identification of r_{eff} and, through the definitions of Laplace pressure (eq 2) and the equilibrium condition (eq 1), the disjoining pressure. Figure 6 shows several typical sets of experimental data for silicon and hard disk substrates that are compared to the force curves calculated using the constant r_{eff} meniscus geometry model described in the previous work.[10] In this plot, increasing force curve length corresponds to decreasing disjoining pressure. Comparison of the two data sets reveals that the force curves performed on the hard drive surface are shorter than curves pulled from silicon surfaces with similar lubricant thicknesses. The higher disjoining pressures associated with the hard drive surface can be attributed to the conductive magnetic layer and the semiconductive diamond overcoat, both of which are more polarizable than the comparable silicon and silicon oxide layers of the silicon wafer. Since these layers are more polarizable, induced dipole−dipole interactions will be stronger for the hard drive surface and will lead to larger dispersive interactions.

Figure 7 displays this difference between the two substrates more clearly by showing disjoining pressure values as a function of lubricant film thickness. The experimental data is compared to the results of Lifshitz theory models for each surface. In these calculations, imaginary dielectric functions for the lubricant and native oxide layer present on the silicon wafers (modeled as

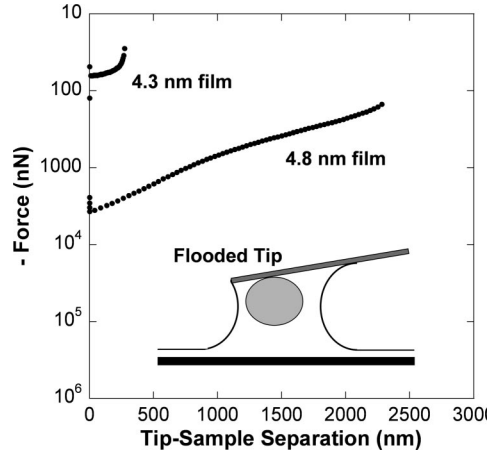

Figure 4. Pull-off force curves for two PFPE films of differing thickness deposited on carbon-coated hard disks. Both curves were performed with the same AFM tip at a retraction velocity of 0.0547 nm/s following a wetting period of 30 min. The increased capillary force and curve length of the 4.8 nm film is attributed to a condition referred to as tip flooding demonstrated in the inset.

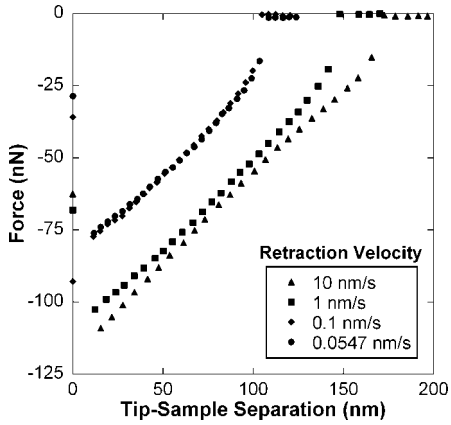

Figure 5. AFM data from a 1.8 nm PFPE film deposited on silicon acquired following a wetting period of 30 min. Changes in curve length and shape are due to variations in constant pull-off velocity during the force curve. Decreasing the velocity results in shorter curves because of the longer time the meniscus has to drain.

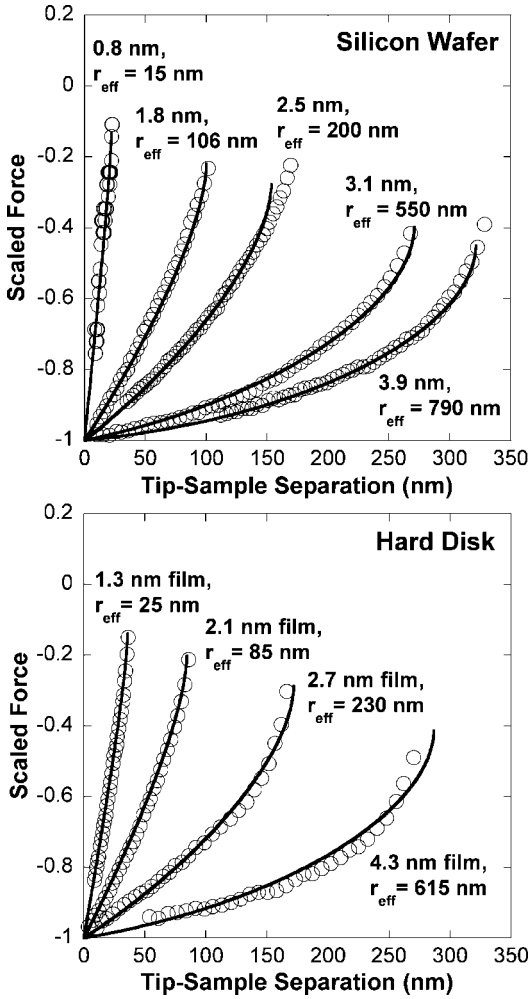

Figure 6. AFM retraction force curves (circles) obtained by stretching Fomblin Z03 from the two surfaces under near equilibrium conditions. The data is scaled with respect to its capillary force at tip−sample contact and fitted with theoretical curves (solid lines) to get the Laplace pressure for each stretched meniscus. The associated film thickness and calculated meniscus radius are presented above each curve.

silica) were approximated using the Ninham−Parsegian method by considering relaxations in the IR and UV.[38,39] A large range of spectroscopic data is available for silicon, and this was transformed into $\varepsilon(i\xi)$ using the Kramers−Kronig relation.[38,40]

Table 1. Dipping Conditions for Film Deposition and Measured Film Thickness

substrate	conc (g PFPE/L solution)	dipping speed (mm/min)	film thickness (nm)
silicon	1.0	85	0.81 ± 0.04
silicon	2.2	40	1.44 ± 0.05
silicon	3.0	40	1.80 ± 0.18
silicon	2.0	85	2.46 ± 0.12
silicon	4.0	45	3.13 ± 0.13
silicon	5.0	60	3.87 ± 0.14
carbon overcoat	1.0	58	0.77 ± 0.07
carbon overcoat	2.0	44	1.32 ± 0.06
carbon overcoat	2.0	75	1.53 ± 0.08
carbon overcoat	5.0	35	1.96 ± 0.15
carbon overcoat	4.0	60	2.08 ± 0.04
carbon overcoat	5.0	55	2.71 ± 0.08
carbon overcoat	5.0	85	3.53 ± 0.04
carbon overcoat	7.1	75	4.28 ± 0.10

The dielectric functions for the nickel−phosphorus (modeled solely as Ni) and cobalt−chromium (modeled exclusively as Co) layers of the hard drive disk were assembled using the methodology of Dagastine et al.[33,34,40−43] The carbon overcoat was modeled as both diamond and a more traditional carbon overcoat. The $\varepsilon(i\xi)$ functions of both were created from published data and the Kramers−Kronig equations.[44]

Table 1 shows the dipping conditions for the various samples used in these experiments along with the measured mean film thickness and standard deviation of the data points. The horizontal error bars displayed in Figure 7 are based upon the standard deviation of the ellipsometry measurements. Vertical error bars are derived from uncertainty in the curve fitting procedure. The criterion for identifying uncertainty in r_{eff} was selecting theoretical curves such that no experimental data points past 20% of the length of the pull-off curve would fall outside the bounds established by the theoretical minimum and maximum curves. Disjoining pressure error calculated in this way was between 6 and 18% of the $\Pi(h)$ value except for the 0.8 nm Z03 on silicon film (36.4%).

Figure 7 reveals the effect of substrate on the disjoining pressure curves. It also displays excellent agreement between the experimental silicon data and its theoretical curve. However, the hard disk data is shifted below the carbon overcoat curve used to model that system. It was thought that this was due to the diamondlike character of the carbon overcoat. Modeling the overcoat exclusively as diamond did improve the fit somewhat but not far enough for it to fit the data as well as the silicon model.

One possible explanation for this persistent shift in the hard disk data was that our selection of 10 nm for the thickness of the magnetic media (from a manufacturer reported range of 10−20 nm) was incorrect and allowing the NiP layer undue influence in the calculation. In Figure 8, a series of Hamaker functions from Lifshitz theory are presented for varying magnetic layer thicknesses and a constant diamond overcoat thickness of 4 nm.

(38) Palik, E. D. *Handbook of Optical Constants*; Academic Press: San Diego, CA, 1992.
(39) Ninham, B. W.; Parsegian, V. A. *Biophys. J.* **1970**, *10*, 646–663.
(40) Dagastine, R. R.; Prieve, D. C.; White, L. R. *J. Colloid Interface Sci.* **2000**, *231*, 351–358.
(41) Crone, R.; Dagastine, R. R.; White, L. R.; Jones, P. M.; Hsia, Y.-T. *Appl. Phys. Lett.* **2006**, *88*, 022509-1–3.
(42) Dagastine, R. R.; Prieve, D. C.; White, L. R. *J. Colloid Interface Sci.* **2002**, *249*, 78–83.
(43) White, L. R.; Dagastine, R. R.; Jones, P. M.; Hsia, Y.-T. *J. Appl. Phys.* **2005**, *97*, 104503-1–7.
(44) Kovarik, P.; Bourbon, E. B.; Prince, R. H. *Phys. Rev. B* **1993**, *48*, 12123–12129.

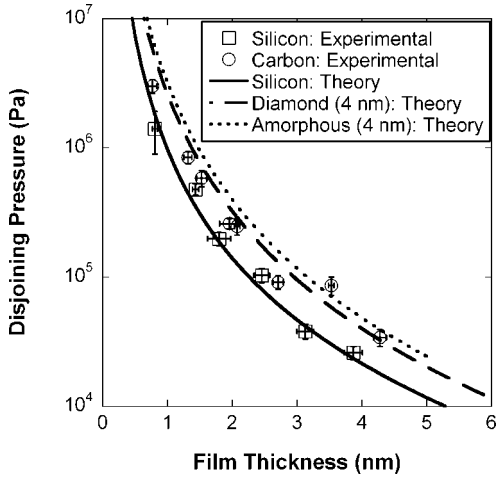

Figure 7. Disjoining pressures calculated via AFM for Fomblin Z03 on silicon wafers and hard drive platters are presented as square and circular icons, respectively. These data sets are compared to Lifshitz theory calculations for a Si/SiO2 surface and two layered hard drive stratigraphies: one terminated in a diamond layer and the other an amorphous carbon stratum.

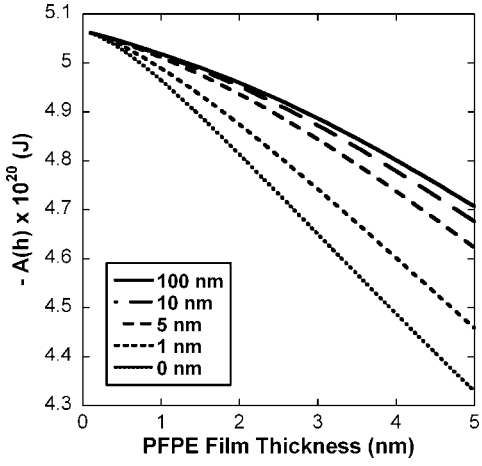

Figure 8. Theoretical Hamaker functions, derived using Lifshitz theory, are displayed for hard disks with varying magnetic media thicknesses (see legend). In each case, a diamond overcoat of 4 nm is assumed to be present above this media.

The plot shows that a 10 nm thick cobalt layer shields the vast majority of the effect of the NiP stratum over the PFPE thicknesses examined in this experiment (via comparison with the 100 nm curve). Increasing the thickness of this layer to 20 nm would have a marginal effect.

Figure 9 examines the effect of using an inaccurate overcoat thickness. In this case, the thickness of the cobalt layer was held constant at 10 nm and the thickness of the overcoat was changed. Incrementally changing the thickness of the overcoat is only effective for shifting the Hamaker function and disjoining pressure curves appreciably at film thicknesses below 2 nm. To yield a

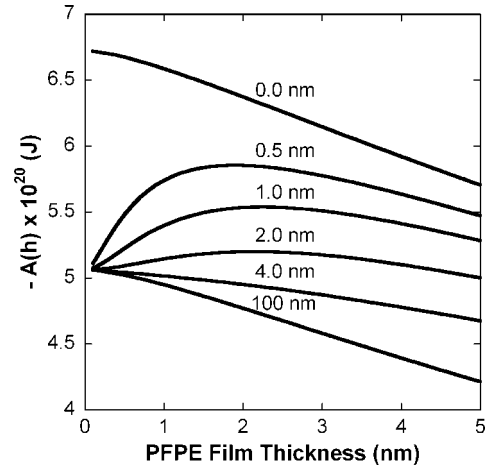

Figure 9. Hamaker functions are plotted for hypothetical hard drive substrates. In each case, a media layer (cobalt) of 10 nm is presumed to be below a diamond overcoat of varying thickness (as shown above the curves).

lower theoretical disjoining pressure curve, the thickness of the overcoat would have to be modeled as larger than 4 nm. However, as Figure 9 reveals, any reasonable increase above 4 nm would shift the $\Pi(h)$ curve negligibly. An additional but uninvestigated reason for the discrepancy is the presence of organic impurities/dopants in the overcoat. Recent research shows that significant oxide layers are present on similar carbon overcoats after exposure to air.[45] The presence of these oxide layers causes very small shifts in the interaction energies of unfunctionalized lubricants on oxidized surfaces (as compared freshly deposited overcoats). These differences could manifest themselves in our DLC disjoining pressure curve and explain the experimental data.

Conclusion

The disjoining pressure of a lubricant film helps establish the protective capacity of that lubricant for the magnetic storage media. We have employed our AFM technique to measure the disjoining pressure of the lubricant Fomblin Z03 on silicon wafers and on an industrially relevant hard drive platter. The AFM method was capable of detecting the effect of changing the substrate. Agreement of the measured disjoining pressure isotherms with Lifshitz theory predictions suggest that interactions in these two systems are primarily from van der Waals forces. The resolution to clearly differentiate between two similar systems bodes well for future studies with this method involving hard drive lubricants having large polar and structural contributions to disjoining pressure.

Acknowledgment. The authors gratefully acknowledge the financial support of Seagate Technology administered through the Data Storage Systems Center at Carnegie Mellon University.

LA8024638

(45) Yun, Y.; Broitman, E.; Gellman, A. J. *Langmuir* **2007**, *23*, 1953–1958.